Supplementary material for "The role of squid for food web structure and community-level metabolism". *Ecological Modelling*

Rémy Denéchère[*, 1, 2], P. Daniël van Denderen[1, 3], and Ken H. Andersen[1]

[1]*Centre for Ocean Life, National Institute of Aquatic Resources (DTU Aqua), Technical University of Denmark, Lyngby, Denmark*

[2]*Scripps Institution of Oceanography, University of California, San Diego, San Diego, CA, United States*

[3]*Graduate School of Oceanography, University of Rhode Island, Narragansett, RI 02882, USA*

[*]*Corresponding author: rdenechere@ucsd.edu; INTEGR OCEANOGRAPHY DIV, Scripps Institution of Oceanography, UC San Diego, 9500 Gilman Drive #0218, La Jolla, CA 92093-0218*

Keywords: FEISTY; squid; fish; food-web; size structure; somatic growth rate

Supplement A Estimation of somatic growth rate.

Cephalopods are usually semelparous (Boyle and Rodhouse, 2008). Their life cycle has two distinct phases: growth and reproduction. They die shortly after reproduction. We assume that the growth curves would fit a von Bertalanffy growth model with a coefficient $k = 0$ (no investment in reproduction) with the following growth in mass per time:

$$\frac{\mathrm{d}m}{\mathrm{d}t} = Am^n,$$

where m is the mass as a function of age t, A the growth coefficient and n the exponent for max. consumption. For the sake of simplicity we assume that $n = 3/4$ similar to fish. Calculation of A can be done with $n = 2/3$ and gives similar results. The above equation assumes that squid invest all their energy in growth and grow exponentially, as observed in our data collection (see SA2). Integrating the above equation over age gives:

$$\int \frac{\mathrm{d}m}{m^n} = \int A\mathrm{d}t$$

$$\left[\frac{m^{1-n}}{1-n}\right]_{M_0}^{m} = [At]_{t_0}^{t},$$

with M_0, the mass at hatching and $t_0 = 0$ the age at hatching. It follows that:

$$m(t)^{1-n} - M_0^{1-n} = (1-n)At$$

$$m(t) = [(1-n)At + M_0^{1-n}]^{1/(1-n)}.$$

For the sake of simplicity we assume that mass at hatching $M_0 \approx 0$. The age dependent mass equation becomes:

$$m(t) \approx [(1-n)At]^{1/(1-n)}. \qquad \text{(SA1)}$$

We collected mass- and length-at-age curves (see Table. SA1) to estimate the somatic growth rate of squid. The body mass metrics in our data collection are expressed in either length l or mass m as a function of age t. To estimate individual somatic growth rate A we converted length to mass from mass at length data collected from (Kooijman, 2009) (Fig. SA1). We assumed that the body length l varies with mass m following: $m = c \times l^b$. We found that length scales with mass with an exponent $b = 2.2$ suggesting that squid does not conserve the same volume structure throughout ontogeny.

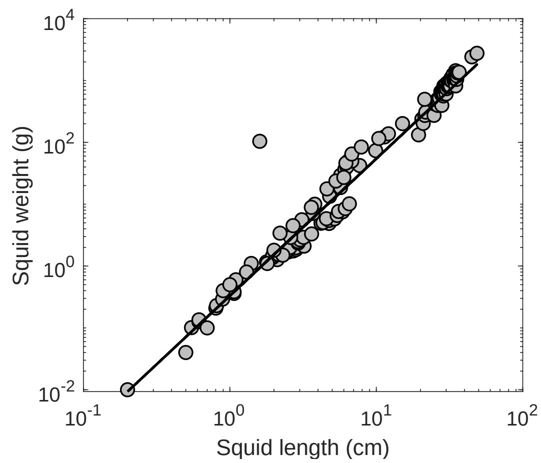

Figure SA1: Relation between mass (g) and length (cm) for squid.

Table SA1: Summary of the data collected on the adult:offspring mass ratio M_∞/M_0 and length at age coefficient, and for the calculation of the somatic growth rate A.

Symbol	Variable	Taxa	Average	Unit	Ref.
Mass at hatching	M_0	squid	0.01	g	(1) & (2)
		Teleost	0.001	g	(2) - (4)
Somatic growth rate	A	squid	23.4	g^{1-n} y^{-1}	(5) - (14)
		Teleost	5	g^{1-n} y^{-1}	(15) & (16)
Length-to-mass coefficient	c	squid	0.33	-	(5) & (17)
Length-to-mass exponent	b	squid	2.2	-	

References: (1) Villanueva et al. (2016); (2) Neuheimer et al. (2015); (3) Denéchère et al. (2022); (4) Andersen (2019); (5) Kooijman (2009); (6) Summers (1971); (7) Pecl (2000); (8) Miyahara et al. (2006); (9) Rodhouse and Hatfield (1990); (10) Agus et al. (2018); (11) Arkhipkin and Silvanovich (1997); (12) Fang et al. (2016); (13) Jackson and Domeier (2003); (14) Rosa et al. (2013); (15) Hutchings et al. (2012); (16) Froese and Pauly (2018); (17) Nabhitabhata (1995).
Note that the above reference for the somatic growth rate A are the reference for the length-at-age or mass-at-age data used for the calculation of A.

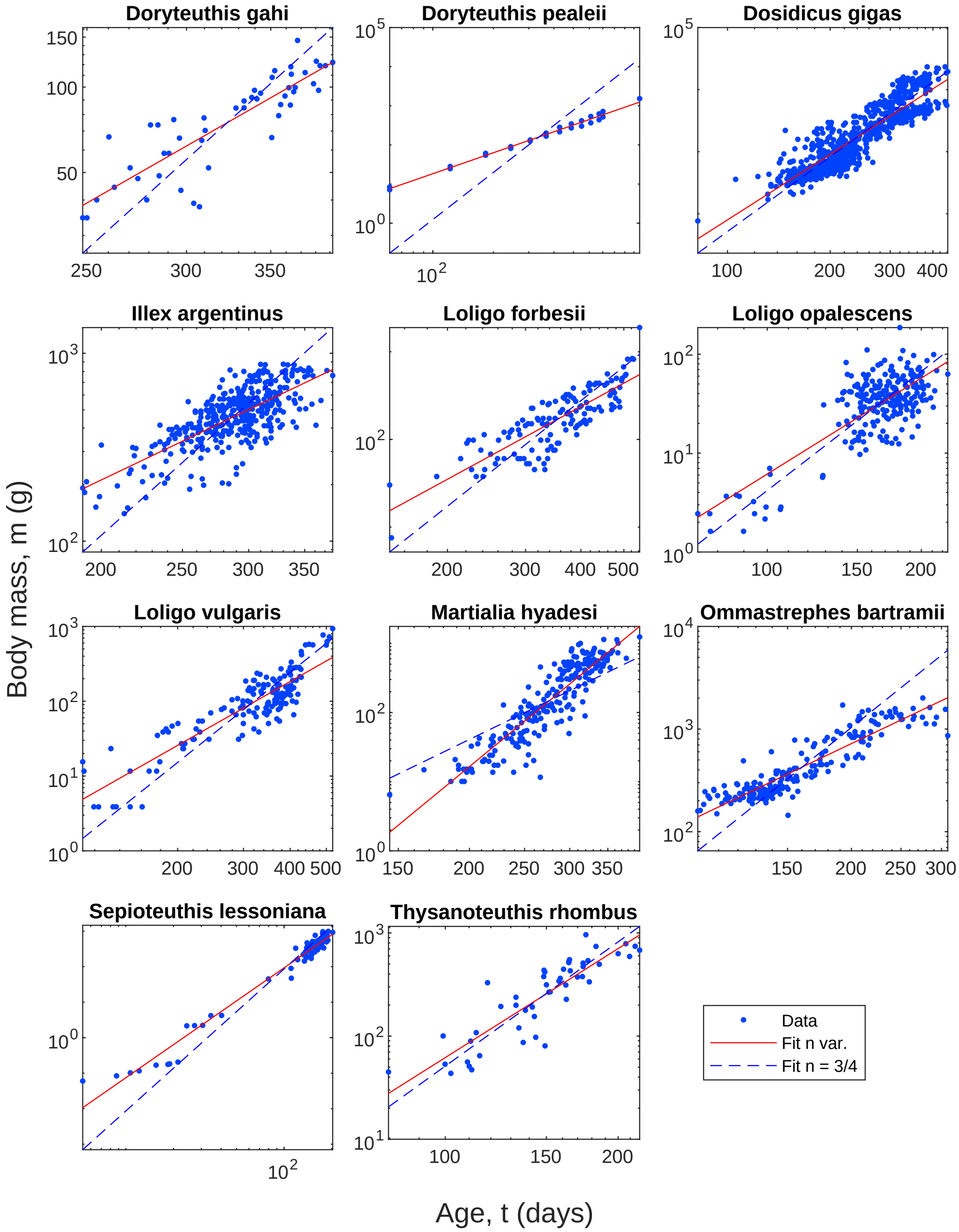

Figure SA2: mass at age data for 11 squid species. The red lines represents the linear regression with n the Exponent for max. consumption as an estimated parameter. The blue dashed line represent the linear regression with fixed Exponent for max. consumption: $n = 3/4$.

Table SA2: Data collected for the somatic growth rate calculation in Fig. SA2

Species	Reference	no.	Location	Sampling period
Doryteuthis gahi	Villegas (2001)	49	Peruvian coast	Nov 1995 - May 1996
Doryteuthis pealeii	Summers (1971)	27	Vineyard Sound	Aug 1967 - July 1970
Dosidicus gigas	Markaida et al. (2004)	396	Gulf of California	Mar - Dec 1996
Illex argentinus	Rodhouse and Hatfield (1990)	344	Patagonia Shelf	Mar 1986 - 1988 & May - Jun 1986
Loligo forbesii		134	Mediterranean Sea	2013 - 2015
Loligo opalescens	Jackson and Domeier (2003)	222	Southern California	Jun 1998 - March 2000
Loligo vulgaris		152	Mediterranean Sea	2013 - 2015
Martialia hyadesi	Arkhipkin and Silvanovich (1997)	225		Apr 1989 - Jun 1990
			Falkland	Jan - Mar 1994
Ommastrephes bartramii	Fang et al. (2016)	161	North Pacific Ocean	July - November 2011
Sepioteuthis lessoniana	Pecl (2000)	76	North & South Australia	Feb 1995 - Oct 1997
Thysanoteuthis rhombus	Miyahara et al. (2006)	49	Sea of Japan	Jan 1999 - Sep 2004

a. Trawl survey

b. Antartic Polar Frontal Zone

Supplement B Main equation of the FEISTY and parameters for the fish functional groups.

Table SB1: Main equation governing the fish in the FEISTY framework. The full description of the Fish model and the governing equations are developed in van Denderen et al. (2020). The following equations are based on a fish size-class i and a prey size-class j.

Description	Equation
Predator:prey interaction	
lower (m_l) and upper (m_u) boundaries of a size-class	$m_{l,i} = m_i/\sqrt{m_i/m_{i+1}}$, $m_{u,i} = m_i/\sqrt{m_i/m_{i+1}}$
Vertical distribution of a predator	$\theta_{z,i}(z,\chi) = \frac{1}{\sqrt{2\pi}\omega_i}\left[\exp\left(-\frac{(z-z_{C1,i,\chi})^2}{2\omega_i^2}\right) + \exp\left(-\frac{(z-z_{C2,i,\chi})^2}{2\omega_i^2}\right)\right]$
	$\theta_{z,i}(z,\chi) = \frac{\theta_{z,i}(z,\chi)}{\sum_z \theta_{z,i}(z,\chi)}$
Width of the vertical distribution	$\omega_i = \omega_0 + \log_{10}(m_i/m_0)\tau$
Predator vertical interaction with prey	$\theta_{v,i,j}(\chi) = \sum_z \min(\theta_{z,i}(z,\chi), \theta_{z,j}(z,\chi))$
Predator:prey size preference	$\theta_{\mathrm{size},i,j} = \sigma\sqrt{\frac{\pi}{2}}\left[\mathrm{erf}\left(\frac{\log(m_{u,i})-\log(m_i)/\beta)}{\sigma\sqrt{2}}\right) - \mathrm{erf}\left(\frac{\log(m_{l,i})-\log(m_i)/\beta)}{\sigma\sqrt{2}}\right)\right]$
Predator feeding preference	$\theta_{i,j} = \theta_{v,i,j} * \theta_{\mathrm{size},i,j}$

Table SB1: Continued

Food encountered	$E_i = V_i \sum_j \theta_{i,j} B_j$
Physiological model of fish	
Search area	$V_i = \gamma m_i^q$
Max. consumption rate	$C_{\max,i} = h m_i^n$
Feeding level	$f_i = E_i/(E_i + C_{\max,i})$
Metabolic rate	$Q_i = \epsilon_\mathrm{a} h f_c m_i^s$
Available energy	$\nu_i = \frac{\kappa_i \nu_i - \delta_i}{1-\alpha_i^{1-\delta_i/(\kappa_i \nu_i)}}$ if $\nu_i > 0$, else 0
Population dynamic	
Flux out size class	$F_i = \epsilon_\mathrm{r}(\gamma_{i^+} B_{i^+} + \sum_{i \in A} \rho_i B_i)$ if $i = 1$, else $\gamma_{i-1} B_{i-1}$
Reproductive output	$\rho_i = (1-\kappa)\nu_i$
Mortality	$\delta_i = \delta_{p,i} + \delta_b$
Predation mortality	$\delta_{p,i} = \sum_i V_i \theta_{i,j} B_i \frac{C_{\max,i}}{E_i, C_{\max,i}}$
Fish Biomass	$\frac{\mathrm{d}B_i}{\mathrm{d}t} = F_i + (\nu_i - \delta_i - \gamma_i - \rho_i) B_i$
Resource biomass	$\frac{\mathrm{d}R_i}{\mathrm{d}t} = r(R_{\max,i} - R_i) - \delta_p, i R_i$
Benthic productivity	$r R_{\max,B} = \epsilon_\mathrm{t}(\min(F_\mathrm{flux}, F_\mathrm{flux} \left(\frac{z_\mathrm{b}}{z_{eu}}\right)^p))$

Table SB2: Parameters for fish in the FEISTY framework.

Symbol	Description	Value	Unit
	Predator:prey interaction		
β	Preferred predator:prey mass ratio	400^{*}	-
σ	Width of the size preference	1.3	-
z_{C}	Depth at maximum concentration	var.$^{a\ *}$	m
z_{b}	Seafloor depth	var.	m
z	Depth	var.	-
γ_0	Smallest width of vertical distribution	10	-
τ	Rate of width increase in vertical distribution	10	-
w_0	Smallest central size	4.5×10^{-5}	g
α	Ratio between individual mass at the lower (m_i) and upper (m_i) boundary of a size class	0.045	-
	Physiological model of fish		
γ	Factor for search area	70	$\mathrm{m}^2\ \mathrm{g}^{-q}\ \mathrm{yr}^{-1}$
q	Exponent for search area	0.8	-
h	Factor for max. consumption rate	20^{*}	$\mathrm{g}^n\ \mathrm{yr}^{-1}$
n	Exponent for max. consumption	3/4	-
b	Factor for metabolic loss	4	$\mathrm{g}^s\ \mathrm{yr}^{-1}$
s	Exponent for metabolic loss	0.85	-
ϵ_{a}	Assimilation efficiency	0.7	-
κ	Fraction of energy used for somatic growth	1 or 0.5	-
	Community-level		
ϵ_{r}	Reproduction efficiency	0.01	-
μ_b	Background mortality	0.1	yr^{-1}

Table SB2: Continued.

M_0	Mass at hatching	0.001 *	g
M_m	Mass at maturation	0.5 or 250 [b]	g
M_∞	Maximum mass	250 or 125000 [b] *	g
	Resource		
R	Biomass of zooplankton and benthos	var.	g m^{-2}
r	Resource turnover rate	1	yr^{-1}
$R_{\max,P}$	Resource carrying capacity		
F_{flux}	Detritial export out of euphotic zone	var.	g m^{-2} yr^{-1}
ϵ_t	Transfer efficiency from detritus to benthos	0.1	-
p	Power law for remineralisation in water column	-0.86	

a. z_C varies per functional group, see our Fig. 2 for the average vertical position of each group and van Denderen et al. (2021, Supplement Table. 1)

b. Value for small and large functional groups

* value that differs for squid

Supplement C Cephalopods in Ecopath

We have reviewed data from seven Ecopath models that include cephalopods in the analysis (Table. SC1). For each model we classified the species or group in different functional group that correspond to the FEISTY functional group – Zooplankton, pelagic, demersals, and cephalopods. We reported the ratio of cephalopod biomass B_{ceph} vs pelagic fish B_{pel} estimated from Ecopath models, i.e., $B_{\text{ceph}}/(B_{\text{ceph}} + B_{\text{pel}})$. The zooplankton productivity (g m^{-2} yr^{-1}) is calculated as product of the production rate over biomass (P/Q in yr^{-1}) and the biomass of zooplankton (g m^{-2}).

Table SC1: Ecopath models including cephalopods.

ID	Maximum depth	Region	Ecosystem type	Reference
438	1000	South East Alaska	Continental shelf	Guénette et al. (2006)
443	2000	West Scotland	Open ocean	Howell et al. (2009)
448	150	Irish Sea	Continental shelf	Lees and Mackinson (2007)
485	500	South Benguela	Upwelling	Shannon et al. (2003)
733	600	Celtic Sea-Biscay	Continental shelf	Bentorcha et al. (2017)
735	200	Celtic Sea	Continental shelf	Moullec et al. (2017)
738	5000	Azores	Open ocean	Morato et al. (2016)

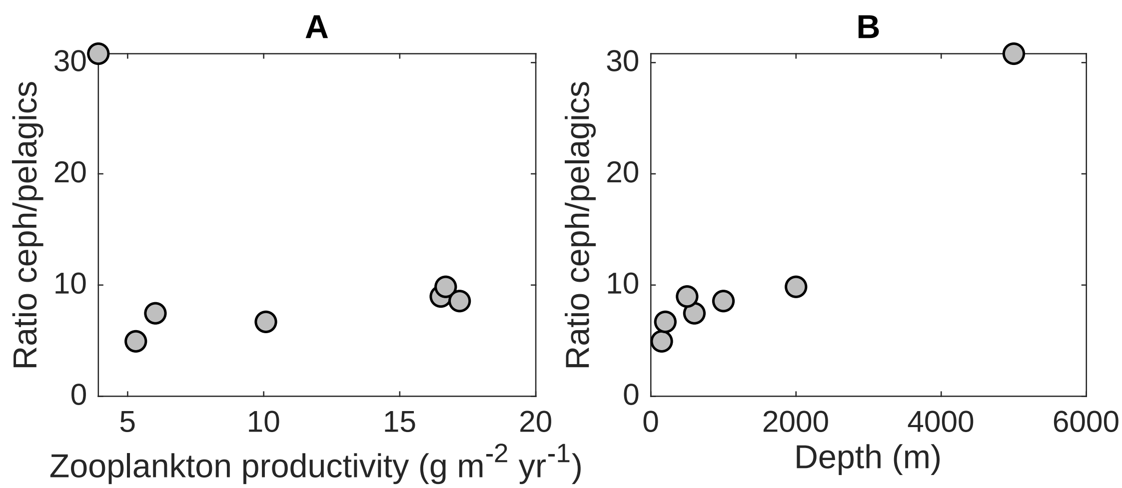

Figure SC1: Ratio of cephalopods vs pelagic (in percent) in Ecopath models with secondary production (A) and depth (B)

Supplement D Effect of predation by squid in FEISTY

The decline of total biomass due to the presence of squid (Fig. 4A & B) is not explained by competition in our model. Their presence results in similar feeding levels for demersal and small pelagic in shelf regions (Fig. **??**C and E) and for small pelagic and large pelagic in the open ocean (Fig. **??**F and H). We further show that increasing the intensity of predation from squid on pelagic groups – small and large – and demersal has a strong effect on other group biomass and total biomass in the system (Fig. SD1). We also show that increasing

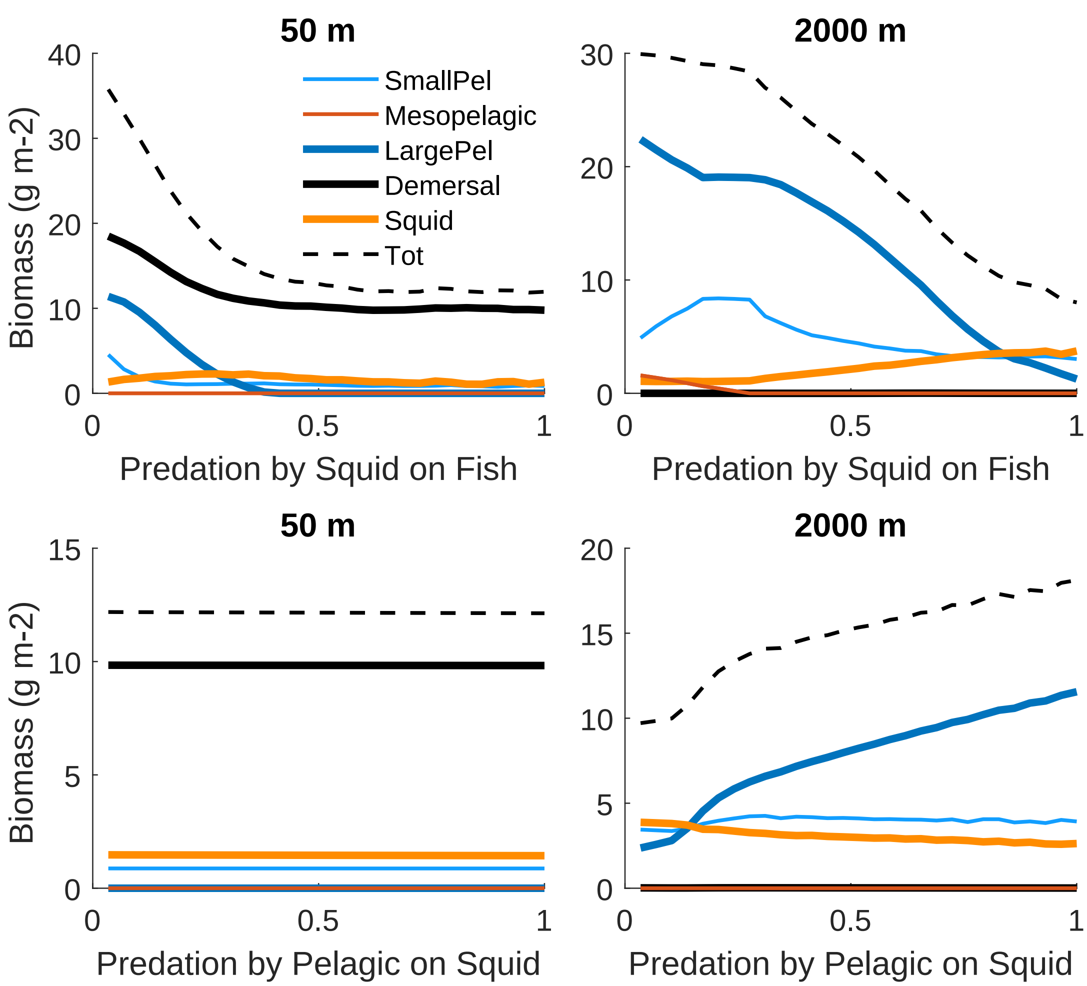

Figure SD1: Effect of squid efficiency to prey on pelagic fish (epipelagic fish and large pelagic) and demersal. Efficiency of predation ranges from 0, no predation to 1, predation depends only on the size- and vertical- overlap of squid and their prey. Simulation has been realised at 50, 2000 meters at a zooplankton productivity of 100 g m^{-2} yr^{-1}.

predation on pelagic in open ocean results in a change in the composition of the system from a dominant of both large and small pelagic to a system dominated by epipelagic fish (Fig. SD1B).

Supplement E Food-web structure without squid.

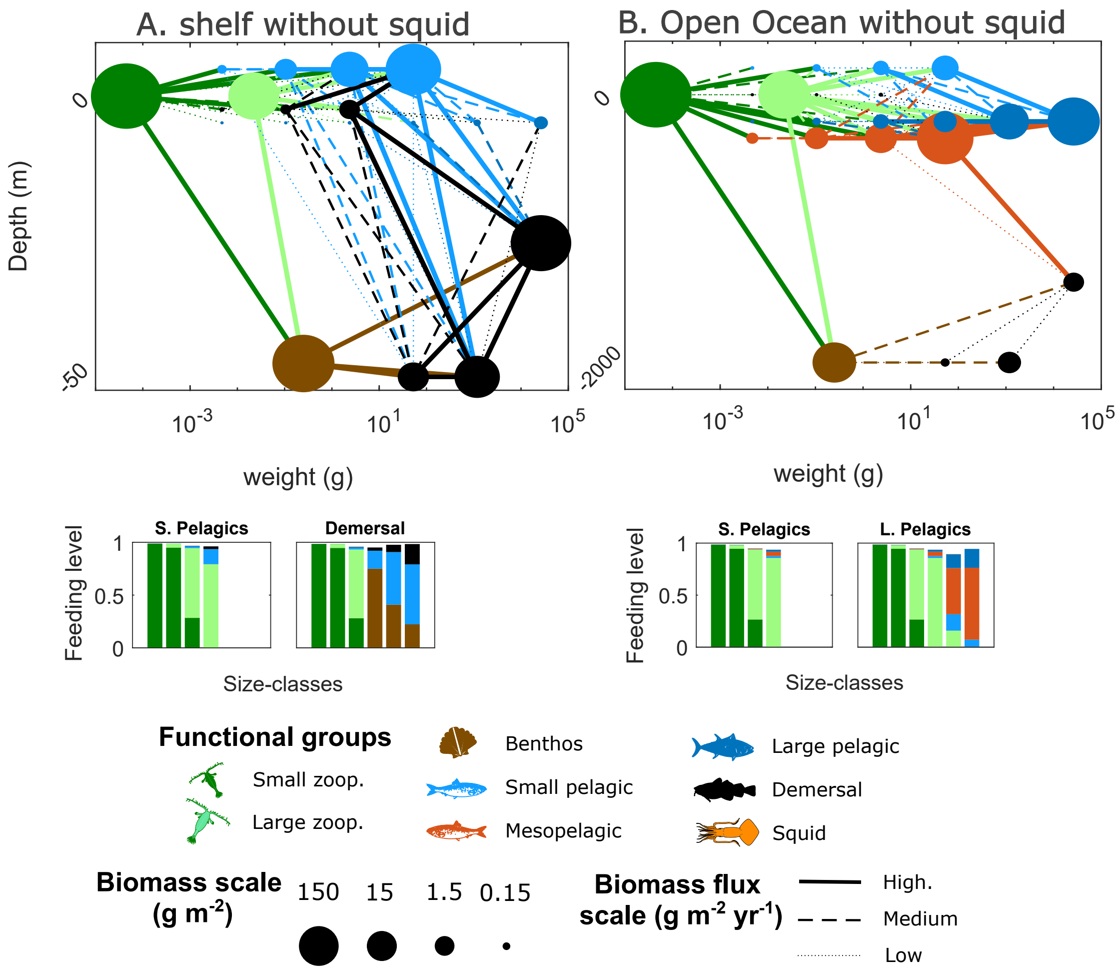

Figure SE1: Comparison of the food-web structure (top panels) and feeding levels (bottom panels) for a shelf (50 m depth) and an open ocean (2000 m depth) system simulated without squid. Dots width in the food-web panel A & B represents the biomass of each functional group: small and large zooplanktons (light and dark green, respectively), benthos (brown), small and large pelagics (light and dark blue, respectively), demersal (black) and squid (orange). Lines represent the biomass flux of prey consumed by a predator. The colors of the biomass fluxes represent the color of the functional type preyed. Feeding levels f (eq. **??**) of small pelagic (light blue), demersal (black), and squid (orange) are presented for the shelf system, and small pelagic, large pelagic, and squid for an open ocean system. All the simulations are made for a zooplankton production of 130 g m^{-2} yr^{-1}. For the sake of simplicity, we only represent the 75 highest fluxes in each food web plot, and scale from low (dotted lines), to medium (dashed lines) to high (plain lines). The biomass of each functional group is plotted over a logarithmic scale to enhance visualization.

Supplement F Effect of predator:prey mass ratio σ, maximum mass M_∞, and somatic growth A on the FEISTY simulation

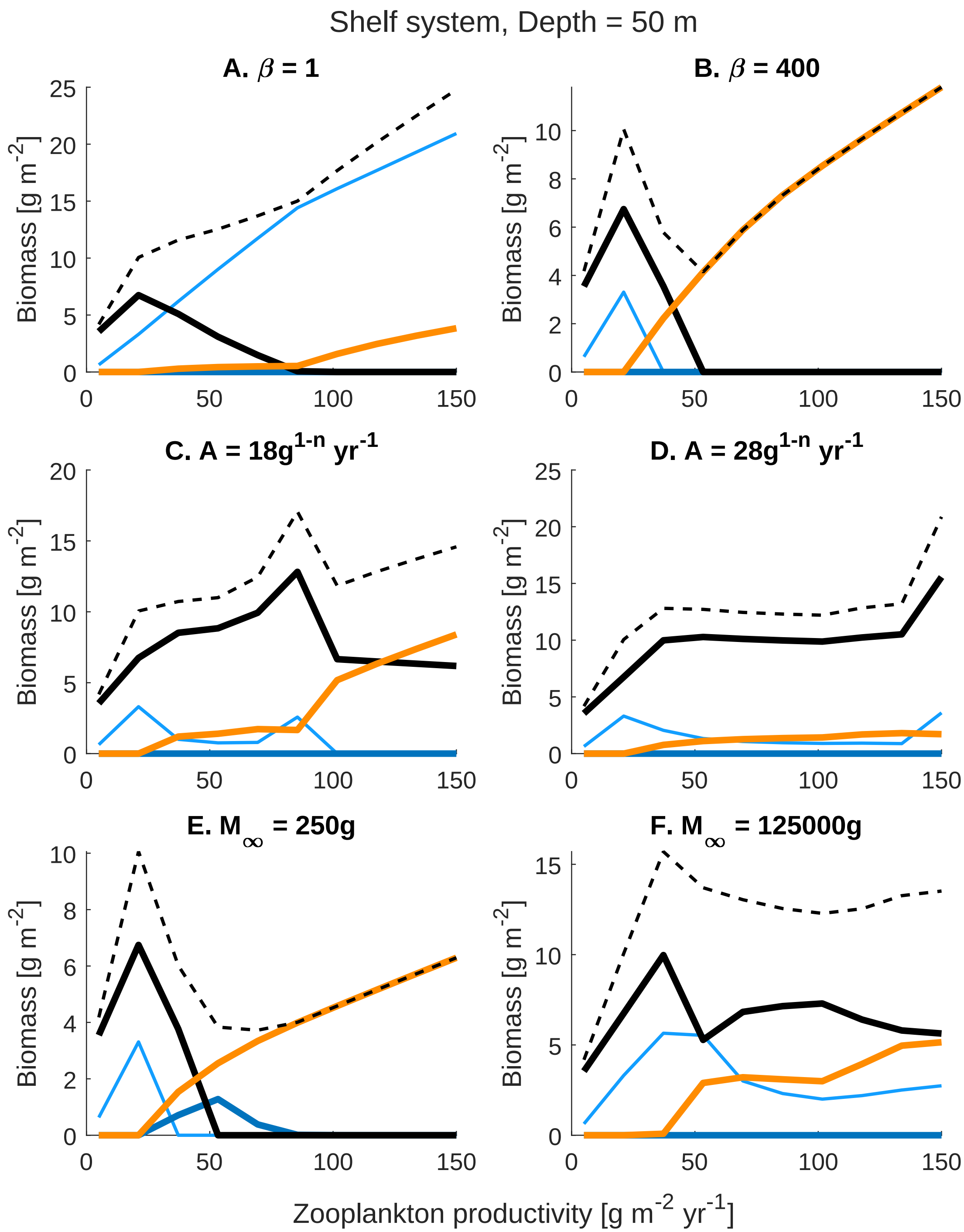

Figure SF1: Sensitivity analysis of the FEISTY-squid framework in a shelf system (50m). We simulated FEISTY-squid with different values of predator:prey size ratio β (A & B), somatic growth rate A (C & D), and maximum size M_∞ (E & F). For β, we used the value estimated for fish (β = 40) and the value estimated from Hoving and Robison (2016). We varied A of about 25% of the value we estimated. We used value of forage fish (250 g) and large pelagics (125000 g) for the maximum mass.

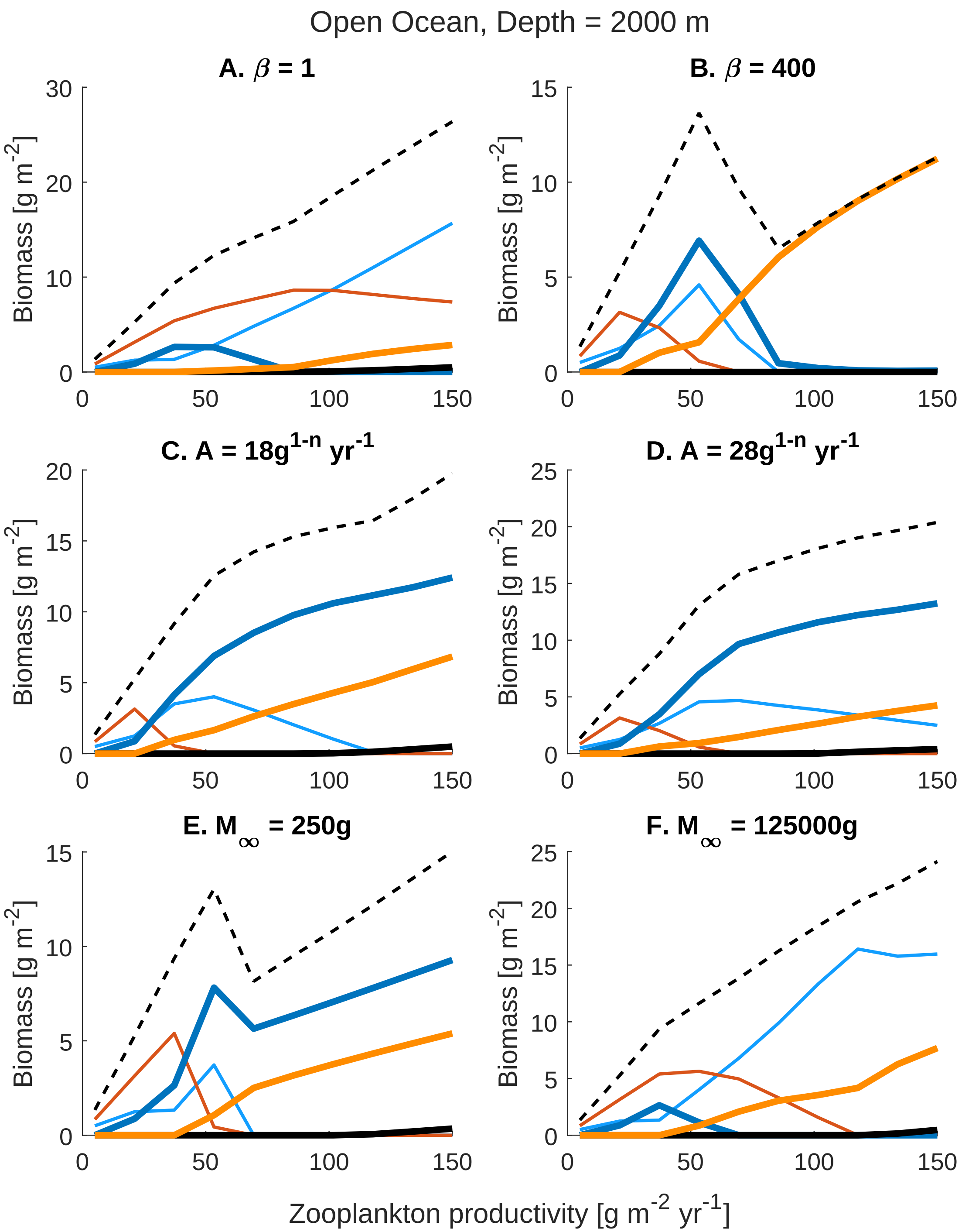

Figure SF2: Sensitivity analysis of the FEISTY-squid framework in the Open Ocean (2000m). We simulated FEISTY-squid with different values of predator:prey size ratio β (A & B), somatic growth rate A (C & D), and maximum size M_∞ (E & F). For β, we used the value estimated for fish (β = 40) and the value estimated from Hoving and Robison (2016). We varied A of about 25% of the value we estimated. We used value of forage fish (250 g) and large pelagics (125000 g) for the maximum mass.

References

Agus, B., M. Mereu, R. Cannas, A. Cau, E. Coluccia, M. C. Follesa, and D. Cuccu (2018). Age determination of loligo vulgaris and loligo forbesii using eye lens analysis. *Zoomorphology 137*(1), 63–70.

Andersen, K. H. (2019). *Fish ecology, evolution, and exploitation: A New Theoretical Synthesis*. Princeton University Press.

Arkhipkin, A. I. and N. V. Silvanovich (1997). Age, growth and maturation of the squid martialia hyadesi (cephalopoda, ommastrephidae) in the south-west atlantic. *Antarctic Science 9*(4), 373–380.

Bentorcha, A., D. Gascuel, and S. Guénette (2017). Using trophic models to assess the impact of fishing in the bay of biscay and the celtic sea. *Aquatic Living Resources 30*, 7.

Boyle, P. and P. Rodhouse (2008). *Cephalopods: ecology and fisheries*. John Wiley & Sons.

Denéchère, R., P. D. van Denderen, and K. H. Andersen (2022). Deriving population scaling rules from individual-level metabolism and life history traits. *The American Naturalist 199*(4), 564–575.

Fang, Z., J. Li, K. Thompson, F. Hu, X. Chen, B. Liu, and Y. Chen (2016). Age, growth, and population structure of the red flying squid (ommastrephes bartramii) in the north pacific ocean, determined from beak microstructure. *Fishery Bulletin 114*(1).

Froese, R. and D. Pauly (2018). FishBase. *World wide web electronic publication. www.fishbase.org*.

Guénette, S., S. J. Heymans, V. Christensen, and A. W. Trites (2006). Ecosystem models show combined effects of fishing, predation, competition, and ocean productivity on steller sea lions (eumetopias jubatus) in alaska. *Canadian Journal of Fisheries and Aquatic Sciences 63*(11), 2495–2517.

Hoving, H.-J. T. and B. Robison (2016). Deep-sea in situ observations of gonatid squid and their prey reveal high occurrence of cannibalism. *Deep Sea Research Part I: Oceanographic Research Papers 116*, 94–98.

Howell, K., S. Heymans, J. Gordon, M. Ayers, and E. Jones (2009). *DEEPFISH Project: Applying an ecosystem approach to the sustainable management of deep-water fisheries. Part 1: Development of an Ecopath with Ecosim model and Part 2: A new aproach to managing deep-water fisheries*. Number 259a, 259b in SAMS Internal reports. Scottish Association for Marine Science. Pages 116 Publisher SAMS Report no. 259.

Hutchings, A. J., R. A. Myers, B. V. García, O. L. Lucifora, and A. Kuparinen (2012). Life-history correlates of extinction risk and recovery potential. *Ecological Applications 22*(4), 1061–1067.

Jackson, G. and M. Domeier (2003). The effects of an extraordinary el niño/la niña event on the size and growth of the squid loligo opalescens off southern california. *Marine Biology 142*(5), 925–935.

Kooijman, S. A. L. M. (2009). *Dynamic Energy Budget Theory for Metabolic Organisation*. New York: Cambridge University Press.

Lees, K. and S. Mackinson (2007). An ecopath model of the irish sea: ecosystems properties and sensitivity analysis. *Sci. Ser. Tech Rep.*.

Markaida, U., C. Quiñónez-Velázquez, and O. Sosa-Nishizaki (2004). Age, growth and maturation of jumbo squid dosidicus gigas (cephalopoda: Ommastrephidae) from the gulf of california, mexico. *Fisheries Research 66*(1), 31–47.

Miyahara, K., T. Ota, T. Goto, and S. Gorie (2006). Age, growth and hatching season of the diamond squid thysanoteuthis rhombus estimated from statolith analysis and catch data in the western sea of japan. *Fisheries Research 80*(2-3), 211–220.

Morato, T., E. Lemey, G. Menezes, C. K. Pham, J. Brito, A. Soszynski, T. J. Pitcher, and J. J. Heymans (2016). Food-web and ecosystem structure of the open-ocean and deep-sea environments of the azores, ne atlantic. *Frontiers in Marine Science 3*, 245.

Moullec, F., D. Gascuel, K. Bentorcha, S. Guénette, and M. Robert (2017). Trophic models: What do we learn about celtic sea and bay of biscay ecosystems? *Journal of Marine Systems 172*, 104–117.

Nabhitabhata, J. (1995, 01). Mass culture of cephalopods in thailand. *World Aquaculture 26*, 25–29.

Neuheimer, A. B., M. Hartvig, J. Heuschele, S. Hylander, T. Kiørboe, K. H. Olsson, J. Sainmont, and K. H. Andersen (2015). Adult and offspring size in the ocean over 17 orders of magnitude follows two life history strategies. *Ecology 96*(12), 3303–3311.

Pecl, G. T. (2000). *Comparative life history of tropical and temperate Sepioteuthis squids in Australian waters*. Ph. D. thesis, James Cook University.

Rodhouse, P. G. and E. Hatfield (1990). Dynamics of growth and maturation in the cephalopod illex argentinus de castellanos, 1960 (teuthoidea: Ommastrephidae). *Philosophical Transactions of the Royal Society of London. Series B: Biological Sciences 329*(1254), 229–241.

Rosa, R., C. Yamashiro, U. Markaida, P. Rodhouse, C. M. Waluda, C. A. Salinas-Zavala, F. Keyl, R. O'Dor, J. S. Stewart, and W. F. Gilly (2013). Dosidicus gigas, humboldt squid.

Shannon, L. J., C. L. Moloney, A. Jarre, and J. G. Field (2003). Trophic flows in the southern benguela during the 1980s and 1990s. *Journal of Marine Systems 39*(1-2), 83–116.

Summers, W. C. (1971). Age and growth of loligo pealei, a population study of the common atlantic coast squid. *The Biological Bulletin 141*(1), 189–201.

van Denderen, D., H. Gislason, J. van den Heuvel, and K. H. Andersen (2020). Global analysis of fish growth rates shows weaker responses to temperature than metabolic predictions. *Global Ecology and Biogeography 29*(12), 2203–2213.

van Denderen, P. D., C. M. Petrik, C. A. Stock, and K. H. Andersen (2021). Emergent global biogeography of marine fish food webs. *Global Ecology and Biogeography 30*(9), 1822–1834.

Villanueva, R., E. A. Vidal, F. Fernández-Álvarez, and J. Nabhitabhata (2016). Early mode of life and hatchling size in cephalopod molluscs: Influence on the species distributional ranges. *PLoS ONE 11*(11), 1–27.

Villegas, P. (2001). Growth, life cycle and fishery biology of loligo gahi (d'orbigny, 1835) off the peruvian coast. *Fisheries Research 54*(1), 123–131.